Journal of Solid State Chemistry **151,** 139–144 (2000)
doi:10.1006/jssc.2000.8636, available online at http://www.idealibrary.com on IDEAL®

Effects of the Oxygen Nonstoichiometry on the Physical Properties of $La_{0.7}Sr_{0.3}MnO_{3-\delta}\square_{\delta}$ Manganites ($0 \leq \delta \leq 0.15$)

N. Abdelmoula, K. Guidara,[1] A. Cheikh–Rouhou, and E. Dhahri

Laboratoire de Physique des Matériaux, Faculté des Sciences de Sfax, BP 802, 3018 Sfax, Tunisia

and

J. C. Joubert

Laboratoire des Matériaux et de Génie Physique, ENSPG, BP 46, 38402 Saint Martin d'Hères, Cedex, France

Received November 8, 1999; in revised form January 19, 2000; accepted January 20, 2000

We present the oxygen deficiency effects on the structural, magnetic, and electrical properties in $La_{0.7}Sr_{0.3}MnO_{3-\delta}\square_{\delta}$ solution where $\square$ is a vacancy and $0 \leq \delta \leq 0.15$. Polycrystalline samples $La_{0.7}Sr_{0.3}MnO_{3-\delta}\square_{\delta}$ were synthesized by a new method. In this series of manganites the Mn^{3+} content is systematically increased due to the increase in the nonstoichiometry δ. X-ray diffraction analysis shows a phase transition from a rhombohedral to an orthorhombic system at $0.075 \leq \delta \leq 0.1$. The material is ferromagnetic for $0 \leq \delta \leq 0.1$ and antiferromagnetic for $0.125 \leq \delta \leq 0.15$. The Curie temperature T_C and saturation magnetization M_s decrease with increasing δ. Resistivity measurements as a function of temperature show a remarkable behavior for the $La_{0.7}Sr_{0.3}MnO_{2.9}$ compound; it is ferromagnetic metallic for $115 \leq T \leq 180$ K and becomes ferromagnetic insulator below 115 K, where a charge ordering seems to appear. The difference in the hopping energies in our samples can be related to the existence of two crystallographic structures, one orthorhombic and the other rhombohedral.

Key Words: **perovskite; manganite; oxygen deficiency.**

I. INTRODUCTION

The number of studies on the doped manganese oxide perovskite compounds, such as $La_{1-x}A_xMnO_3$ where A is a monovalent or a divalent element, has increased dramatically due to the giant magnetoresistance exhibited near the ferromagnetic transition (1–3). The use of these materials in technological applications such as magnetic read–write heads is made possible as a result of their interesting structural, magnetic, and transport properties. It is believed that the stoichiometric compound $LaMnO_3$ (Mn^{3+} $t_{2g}^3 e_g^1$) is antiferromagnetic due to the superexchange coupling between Mn^{3+} ions. The partial substitution on the La^{3+} site by a divalent alkaline earth ion (Sr^{2+}, Ca^{2+}, Ba^{2+}) induces a mixed valence of Mn^{3+} and Mn^{4+} ions. Their interaction is responsible for the metallic and ferromagnetic properties due to the double-exchange mechanism (4). Recent studies show that the Curie temperature T_C related to the mobility of the e_g electrons and the structural transitions are strongly dependent on the mixed valence Mn^{3+}–Mn^{4+}, the externally applied pressure (5), and the size mismatch between A and La (6–10).

The classic methods used to change the Mn^{4+} content involves substituting La^{3+} by a divalent element or creating vacancies in the La, Mn, or O sites in $LaMnO_3$. These vacancies can be obtained by varying the synthesis conditions and subsequent annealing treatments (11–13).

A search for a new method of creating vacancies in the oxygen sites (oxygen content < 3) has been of interest due to the importance of the potential technological applications of these vacancies, such as in a solid oxide fuel combustible (SOFC), high-temperature electrolyzers, oxygen sensors, and catalysis.

In order to clarify the oxygen deficiency effects on the structural, magnetic, and electrical properties, we have prepared a series of samples $La_{0.7}Sr_{0.3}MnO_{3-\delta}\square_{\delta}$ where $\square$ is a vacancy and $0 \leq \delta \leq 0.15$. In this system, the number of Mn^{3+} and Mn^{4+} ions is systematically varied with δ. The developed electronic formula of the samples is

$$La_{0.7}^{3+}Sr_{0.3}^{2+}Mn_{0.7+2\delta}^{3+}Mn_{0.3-2\delta}^{4+}O_{3-\delta}^{2-}\square_{\delta}.$$

Thus, the Mn^{3+} and Mn^{4+} concentrations are respectively $(0.7 + 2\delta)$ and $(0.3 - 2\delta)$.

[1] To whom correspondence should be addressed. Fax: 216 4 274 437; E-mail: KamelGuidara@fss.rnu.tn.

0022-4596/00 $35.00

II. SAMPLE PREPARATION

The nonstoichiometric perovskite oxides $La_{0.7}Sr_{0.3}MnO_{3-\delta}\square_\delta$ were prepared by creating vacancies in the oxygen sites in the sample $La_{0.7}Sr_{0.3}MnO_3$ according to the equation

$$La_{0.7}Sr_{0.3}MnO_3 + \frac{\delta}{2}Ti \rightarrow \frac{\delta}{2}TiO_2 + La_{0.7}Sr_{0.3}MnO_{3-\delta}\square_\delta. \quad [1]$$

The parent oxide $La_{0.7}Sr_{0.3}MnO_3$ was synthesized by the standard solid-state reaction. The precursors La_2O_3, $SrCO_3$, and MnO_2 of high purity (more than 99%) powders were fired in air at 673 K for 12 h before being used. Those materials were thoroughly mixed in an agate mortar in stoichiometric proportions and heated at 1173 K for 3 days with an intermediate regrinding. The resulting powder was pressed into pellets under 4 tons/cm^2 and fired at 1673 K for 2 days in air with several periods of grinding and repelleting. Finally these pellets were rapidly quenched to room temperature. This step was carried out in order to keep the structure at an annealed temperature. The sample was next placed in a quartz tube containing titan in the stoichiometric proportion of Eq. [1]. The tube was pumped, sealed, and annealed at 973 K for 1 week.

The nonstoichiometry parameter δ was checked by chemical titration. The samples was dissolved in an excess of VO^{2+} in sulfuric acid and titrated with $KMnO_4$ solution (14).

The phase purity, structure, and lattice parameters of the samples were determined by X-ray powder diffraction with Cr$K\alpha_1$ radiation at room temperature. High-purity silicon powder was used as an internal standard. Unit cell parameters were obtained by least-squares calculations.

The magnetization M of the samples as a function of temperature under 500 Oe was obtained using a home-built Faraday-type balance for $\delta \leq 0.025$ and a Foner magnetometer equipped with a superconducting coil for $\delta > 0.025$.

Resistivity measurements were performed using the conventional four-probe method in the earth's magnetic field.

III. RESULTS AND DISCUSSION

III-1. X-Ray Characterization

X-ray patterns at room temperature of some samples are shown in Fig. 1. All samples are in a single phase. For $\delta \leq 0.075$ the structure is rhombohedral. It becomes orthorhombic for $\delta \geq 0.1$. The crystallographic data are listed in Table 1. The unit cell volume V increases with the δ vacancy rate (Fig. 2). The increase of the unit cell volume can be attributed to two factors:

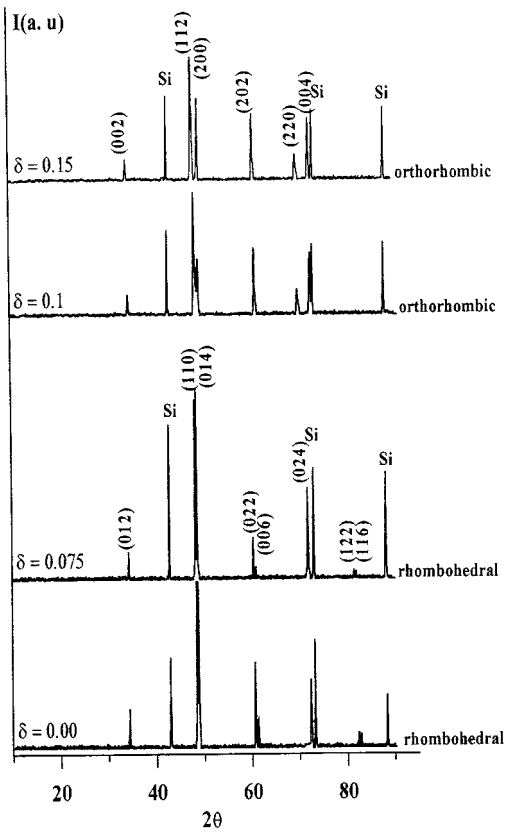

FIG. 1. X-ray diffraction powder patterns for some perovskite $La_{0.7}Sr_{0.3}MnO_{3-\delta}\square_\delta$ samples.

(i) the reduction of Mn^{4+} to Mn^{3+} with greatest ionic radii and

(ii) the reduction of the bending electrostatic forces due to the creation of vacancies at oxygen sites.

At room temperature, all the orthorhombic samples fulfill the criterion $(c/a) < \sqrt{2}$ characteristic of a cooperative Jahn–Teller deformation.

The structural phase transition from rhombohedral to orthorhombic appears at $0.075 \leq \delta \leq 0.1$ corresponding to an Mn^{3+} concentration varying between 85% and 90%. A similar transition from orthorhombic to rhombohedral has been observed by Töpfer and Goodenough in the La and Mn vacancy solution $LaMnO_{3+\delta}$ at $82\% \leq Mn^{3+} \leq 88\%$ ($0.06 \leq \delta \leq 0.09$) (14) and Urishabara *et al.* in the $La_{1-x}Sr_xMnO_3$ system at $82.5\% \leq Mn^{3+} \leq 85\%$ ($0.15 \leq x \leq 0.175$) (15). These solutions undergo a structural phase transition from rhombohedral to orthorhombic at the same Mn^{3+} concentration ($82\% \leq Mn^{3+} \leq 90\%$). Consequently, the structural transition observed in the $La_{0.7}Sr_{0.3}MnO_{3-\delta}\square_\delta$ series is related not to the vacancy site but to the Mn^{3+} concentration which causes a distortion by the Jahn–Teller effect.

TABLE 1
Crystallographic Data of $La_{0.7}Sr_{0.3}MnO_{3-\delta}\square_\delta$ Samples with Mn^{3+} Content

δ	$\%Mn^{3+}$	Structure	Lattice parameters	Unit cell volume V (Å^3)
0.000	70	Rhombohedral	$a_r = 5.46$ Å $\alpha = 60.43°$	58.48
0.025	75	Rhombohedral	$a_r = 5.47$ Å $\alpha = 60.42°$	58.68
0.050	80	Rhombohedral	$a_r = 5.48$ Å $\alpha = 60.40°$	58.89
0.075	85	Rhombohedral	$a_r = 5.49$ Å $\alpha = 60.38°$	59.06
0.100	90	Orthorhombic	$a_o = 5.52$ Å $b_o = 5.62$ Å $c_o = 7.77$ Å	60.34
0.125	95	Orthorhombic	$a_o = 5.51$ Å $b_o = 5.72$ Å $c_o = 7.72$ Å	60.91
0.150	100	Orthorhombic	$a_o = 5.50$ Å $b_o = 5.84$ Å $c_o = 7.68$ Å	61.74

TABLE 2
Transition Temperatures T_N and T_C and Saturation Magnetization M_S Determined at 500 Oe for $La_{0.7}Sr_{0.3}MnO_{3-\delta}\square_\delta$

δ	T_N (K)	T_C (K)	M_S (emu/g)
0.000		365	
0.025		342	
0.050		300	33.6
0.075		215	26.7
0.100		125	23.2
0.125	119		9.12
0.150	110		4.70

III-2. Magnetic Properties

The temperature dependence of magnetization at 500 Oe shows that there is evidence of collinear ferromagnetic alignment of the spins below the Curie temperature for $\delta \leq 0.1$. These materials become antiferromagnetic for $\delta \geq 0.125$ which represents the setting up of an antiferrodistortive Mn^{3+} ($t_{2g}^3 e_g^1$) orbital ordering due to the cooperative Jahn–Teller effect.

We have used the maximum of the slope of $M(T)$ curves as a criterion to determine the magnetic temperature transition. The Curie temperature T_C decreases from 365 to 125 K with increasing δ (Table 2). We note also that the magnitude of the saturation magnetization M_S for $La_{0.7}Sr_{0.3}MnO_{3-\delta}\square_\delta$ samples at 10 K is reduced with increasing oxygen deficiency δ (Table 2). This phenomenon can be interpreted on the basis of the decrease of the number of pairs Mn^{3+}/Mn^{4+} with the increase of δ that causes a reduction of the transfer interaction of e_g electrons. It is therefore likely that in the nonstoichiometric $La_{0.7}Sr_{0.3}MnO_{3-\delta}\square_\delta$ solution, the Curie temperature T_C value is critical to determining the rate of oxygen deficiency δ.

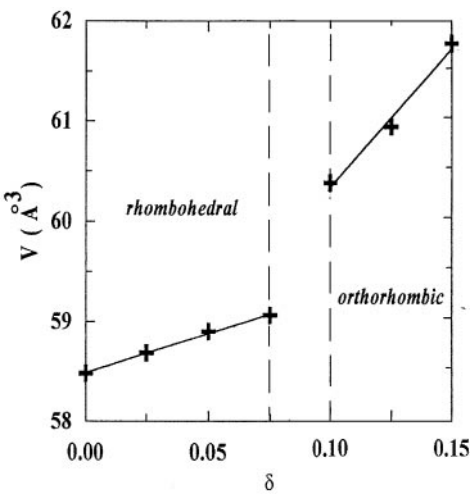

FIG. 2. Variation of the unit cell volume with δ for $La_{0.7}Sr_{0.3}MnO_{3-\delta}\square_\delta$.

In order to study the effect of vacancy on double-exchange energy, we have compared the T_C values of the vacancy solution $La_{0.7}Sr_{0.3}MnO_{3-\delta}\square_\delta$ to the corresponding values of the nonstoichiometric solution $La_{1-x}Sr_xMnO_3$ ($0.0 \leq x \leq 0.6$) (15). The developed electronic formulas of these solutions are respectively

$$La_{1-x}^{3+}Sr_x^{2+}Mn_{1-x}^{3+}Mn_x^{4+}O_3^{2-} \quad [2]$$

$$La_{0.7}^{3+}Sr_{0.3}^{2+}Mn_{0.7+2\delta}^{3+}Mn_{0.3-2\delta}^{4+}O_{3-\delta}^{2-}\square_\delta. \quad [3]$$

As a consequence, for $x = 0.3 - 2\delta$, the preceding solutions have the same Mn^{3+} concentration. We have calculated the ΔT_C divergence as a function of δ defined by the equation

$$\Delta T_C(\delta) = T_C(1,\ x = 0.3 - 2\delta) - T_C(2,\delta),$$

where $T_C(1,\ x = 0.3 - 2\delta)$ and $T_C(2,\ \delta)$ are respectively the Curie temperature for the stoichiometric and nonstoichiometric solutions.

In Fig. 3, we report the variation of $T_C(1)$ and $T_C(2)$ values as a function of Mn^{3+} concentration. These curves show that the Curie temperature has the same behavior in the two solutions. However, in the nonstoichiomeric solution, the T_C values are shifted to low temperatures. We show in Fig. 3 (inset) the evolution of ΔT_C with the rate of oxygen deficiency δ.

The precedent curve shows that the double-exchange energy for a given Mn^{3+} concentration decereses linearly

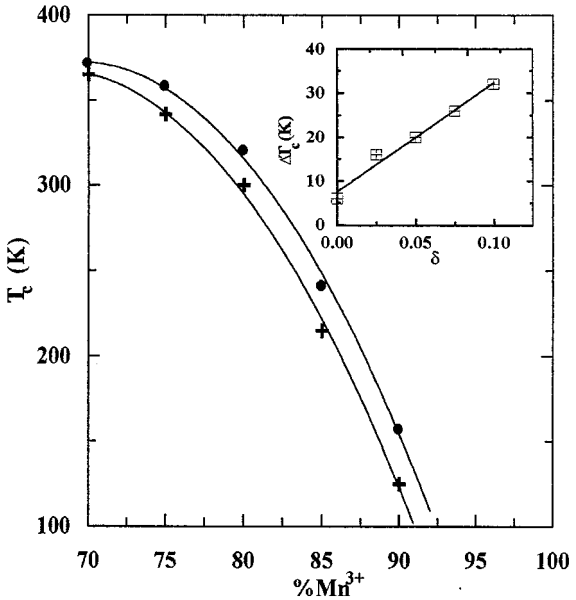

FIG. 3. Variation of T_C as a function of the Mn^{3+} concentration for $La_{0.7}Sr_{0.3}MnO_{3-\delta}\square_\delta$ (+) and $La_{1-x}Sr_xMnO_3$ (●) solutions. Inset: ΔT_C shift of $La_{0.7}Sr_{0.3}MnO_{3-\delta}\square_\delta$ as a function of δ.

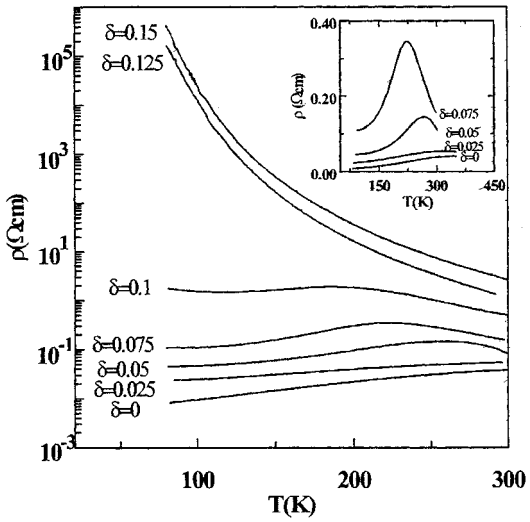

FIG. 4. Temperature dependence of resistivity (ρ) for $La_{0.7}Sr_{0.3}MnO_{3-\delta}\square_\delta$ ($0.0 \le \delta \le 0.15$). Inset: Temperature dependence of resistivity (ρ) for the ferromagnetic samples.

with δ.

$$E_{ex}(x,\delta) = E_{ex}(x) - A\delta \qquad (0 \le \delta \le 0.1)$$

where x is the tetravalent manganese concentration, δ is the vacancy rate, and A is about 2.14 eV (248 K). Therefore, the double-exchange energy is extremely sensitive to the chemical defect in oxygen sites.

III-3. Electrical Properties

The temperature dependences of resistivity $\rho(T)$ for all samples are represented in Fig. 4. Using the sign of the temperature coefficient of resistivity ($d\rho/dT$) as a criterion, we found that for $\delta \le 0.075$, these compounds are ferromagnetic metallic at low temperature ($T < T_p$) and become paramagnetic semiconductor above the temperature peak T_p (Fig. 4 inset). It is also remarkable that the resistivity temperature peak decreases and the resistivity peak ρ_p increases with increasing δ. The structural transition from rhombohedral to orthorhombic suggests that the tilting of the MnO_6 octahedra becomes more important as the vacancy rate increases which causes the reduction of the M_s and T_C values observed in these compounds (16). The sample with $\delta = 0.1$ has an exceptional behavior. It is ferromagnetic insulator at low temperature and becomes ferromagnetic metal between $T_{FM} = 115$ K and $T_p = 180$ K. Above the resistivity peak temperature T_p, this compound is paramagnetic semiconductor. The ferromagnetic insulating state seems to be due to an ordering of the Mn^{3+} and Mn^{4+} species on the manganese lattice, which causes a narrowing of the double-exchange interactions and consequently a very small canting of the ferromagnetic order (Fig. 5). A similar behavior was observed by Urishabara *et al.* (15) in the low doping region of the phase diagram of $La_{1-x}Sr_xMnO_3$ and by Pinsard *et al.* (17) in $La_{0.875}Sr_{0.125}MnO_3$.

For the highest δ values ($\delta = 0.125$, 0.15), the samples have an insulating behavior ($d\rho/dT < 0$) consistent with the antiferromagnetic comportment of these materials (Fig. 4).

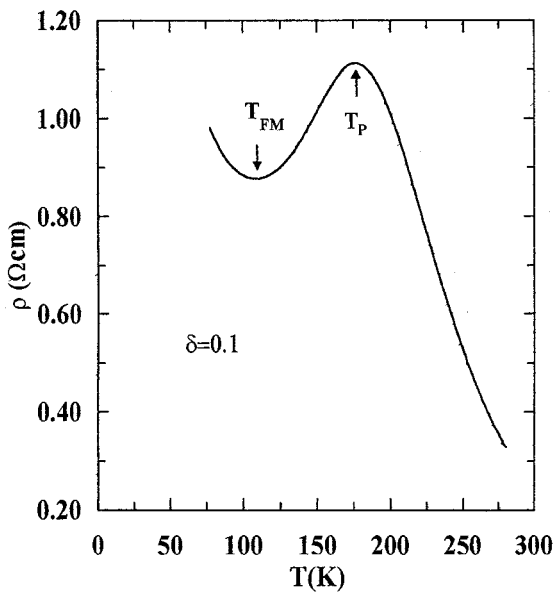

FIG. 5. Resistivity (ρ) of $La_{0.7}Sr_{0.3}MnO_{3-\delta}\square_\delta$ ($\delta = 0.1$) as a function of temperature. Arrows indicate the temperature transitions.

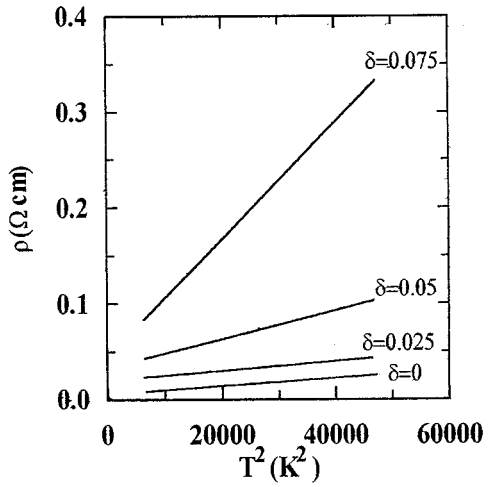

FIG. 6. Temperature dependence of the resistivity in the low-temperature ferromagnetic regime ($T \leq 215$ K) for $La_{0.7}Sr_{0.3}MnO_{3-\delta}\square_\delta$.

In the low-temperature ferromagnetic regime, the temperature dependence of the resistivity for $0 \leq \delta \leq 0.075$ samples is described by a quadratic function (Fig. 6):

$$\rho(T) = \rho(0) + AT^2 \qquad (T \leq 215 \text{ K}).$$

The resistivity seems to be governed by the electron–electron scattering process associated with spin fluctuation (15, 18). The variation of the coefficient A as a function of δ is shown in Fig. 7. It increases exponentially with the increase of the oxygen deficiency δ.

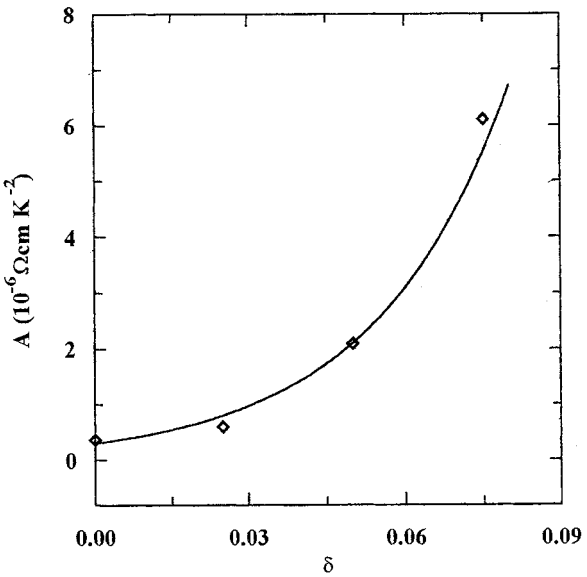

FIG. 7. A coefficient as a function of the vacancy rate δ for $La_{0.7}Sr_{0.3}MnO_{3-\delta}\square_\delta$ ($0.0 \leq \delta \leq 0.075$).

The behavior of the resistivity data above the ferromagnetic transition temperature is indicative of conduction by magnetic polarons. In the samples ($\delta = 0.1, 0.125$, and 0.15), the resistivity in the paramagnetic region fits quite well the function

$$\rho = \rho_0 e^{E_{\text{hop}}/KT}.$$

The hopping energy (E_{hop}) values are respectively 50, 90, and 110 meV. The different E_{hop} values can be related to the existence of a structural transition from rhombohedral to orthorhombic.

IV. CONCLUSION

In this work, we have studied the important role of the oxygen deficiency in determining the structural magnetic and electrical properties of $La_{0.7}Sr_{0.3}MnO_{3-\delta}\square_\delta$ oxides. The unit cell volume increases, mainly caused by a decrease in the Mn^{4+} concentration. This increase, due to the reduction of the material, leads to an orthorhombic–rhombohedral structure change and therefore to a decrease in magnetization and transition temperature T_C. The exchange energy decreases as δ increases. The electrical investigation shows ferromagnetic metallic system for the lowest δ values ($\delta \leq 0.075$) and antiferromagntic insulator system for $\delta \geq 0.125$.

The $\delta = 0.1$ sample has a remarkable behavior explained by a charge ordering mechanism.

The rate of oxygen deficiency δ is critical to the structural, magnetic, and electrical properties of the manganites, and therefore the preparation method should be carefully controlled to obtain samples with the desired T_C and physical properties.

REFERENCES

1. R. Von Helmolt, B. Holzapfel, L. Schultz, and K. Samwer, *Phys. Rev. Lett.* **71,** 2331 (1993).
2. C. Boudaya, L. Laroussi, E. Dhahri, J. C. Joubert, and A. Cheikhrouhou, *J. Phys.: Condens. Matter* **10,** 7485 (1998).
3. E. Dhahri, K. Guidara, A. Cheikh-Rouhou, J. C. Joubert, and J. Pierre, *Phase Transit.* **66,** 99 (1998).
4. C. Zener, *Phys. Rev.* **82,** 403 (1951).
5. Y. Moritomo, H. Kuwahara, Y. Tomioka, and Y. Tokura, *Phys. Rev. B* **55,** 7549 (1997).
6. F. Damay, C. Martin, A. Maignan, and B. Raveau, *J. Appl. Phys.* **82,** 6181 (1997).
7. N. Abdelmoula, E. Dhahri, K. Guidara, and J. C. Joubert, *Phase Transit.* **69,** 215 (1999).
8. C. N. R. Rao, P. N. Santhosh, R. S. Singh, and A. Arulraj, *J. Solid State Chem.* **169,** 135 (1998).
9. A. Sundaresan, P. L. Paulose, R. Mallik, and E. V. Sampathkumaran, *Phys. Rev. B* **57,** 2690 (1998).
10. X. G. Li, X. J. Fan, G. Ji, W. B. Wu, K. H. Wong, C. L. Choy, and H. C. Ku, *J. Appl. Phys.* **85**(3), 1663 (1999).
11. V. A. Cherepanov, L. Yu. Barkhatova, A. N. Petrov, and V. I. Voronin, *J. Solid State Chem.* **118,** 53 (1995).

12. T. R. McGuire, A. Gupta, P. R. Duncombe, M. Rupp, J. Z. Sun, R. B. Laibowitz, and W. J. Gallagher, *J. Appl. Phys.* **79,** 4549 (1996).
13. P. S. I. P. N. de Silva, F. M. Richards, L. F. Cohen, J. A. Alonso, M. J. Martinez-Lope, M. T. Casais, K. A. Thomas, and J. L. MacManus-Driscoll, *J. Appl. Phys.* **83,** 394 (1998).
14. J. Töpfer and J. B. Goodenough, *J. Solid State Chem.* **130,** 117 (1997).
15. A. Urushibara, Y. Moritomo, T. Arima, A. Asamitsu, G. Kido, and Y. Tokura, *Phys. Rev. B* **51,** 14103 (1995).
16. J. Fontcuberta, B. Martinez, A. Seffar, S. Pinol, J. L. Garcia-Munoz, and X. Obradors, *Phys. Rev. Lett.* **76,** 1122 (1996).
17. L. Pinsard, J. Rodriguez-Carvajal, A. H. Moudden, A. Anane, A. Revcolevschi, and C. Dupas, *Physica B* **234,** 856 (1997).
18. Z. Guo, J. Zhang, N. Zhang, W. Ding, H. Huang, and Y. Du, Appl. *Phys. Lett.* **70,** 1897 (1997).